Performance comparison of NRZ, AMI and DPSK modulation schemes in multi-input multi-output mode division multiplexing based radio over FSO transmission system

KARAMJEET SINGH[a,b], AMIT GROVER[b], MEHTAB SINGH[c,d,*], JYOTEESH MALHOTRA[c]
[a]*Department of Electronics and Communication Engineering, IKG-PTU, Kapurthala, India*
[b]*Department of Electronics and Communication Engineering, Shaheed Bhagat Singh State University, Ferozepur, India*
[c]*Department of Engineering and Technology, Guru Nanak Dev University, Regional Campus, Jalandhar, India*
[d]*Department of Electronics and Communication Engineering, SIET, Amritsar (IKG-PTU, Kapurthala), India*

In this research, the performance of a 2×2, 3×3, and 4×4 optical multi-input-multi-output (MIMO) transmission-based radio over free space optics (RoFSO) link using mode division multiplexing (MDM) technique is reported. The link performance is evaluated and compared for non-return to zero (NRZ), differential phase-shift keying (DPSK), and alternate mark inversion (AMI) modulation over varying range of FSO link. Modulation schemes performance has been compared employing the received signal-to-noise ratio (SNR) as the performance metrics. The results exhibit that the DPSK modulation scheme performs the best, followed by AMI and NRZ scheme for all MIMO-MDM-based RoFSO systems. Effective transmission of 40Gbps-80GHz information in clear weather conditions over a 16 km FSO link range with appropriate SNR (> 20 dB) was demonstrated in the MDM-RoFSO transmission system which is based on DPSK modulation. This is a major improvement in information capacity and connectivity compared to previously reported literature.

(Received October 8, 2020; accepted August 16, 2021)

Keywords: MIMO, RoFSO, MDM, Attenuation, Link range

1. Introduction

The transportation of radio frequency (RF) data signals on free space channel, also referred as radio over free space optics (RoFSO) links is being valued as an efficacious and secure means of information transmission due to their numerous merits, including plenty amount of spectrum which is unregulated and does not need licensing, massive channel bandwidth, low beam divergence, high-speed links, narrow beam size, immunity to electromagnetic interference, low-security upgrades, last-mile access, quick and easy deployment, low power consumption, and cost-effectiveness [1, 2]. It finds application in indoor and outdoor information transmission systems viz., inter-satellite links, satellite-to-earth links, deep-space links, earth-to-satellite links, visible light links and terrestrial links [3]. Despite many merits promised by RoFSO links, the main constraint is the attenuation offered because of various atmospheric conditions that limit the link performance. On the other side, for supplementing data transportation in RoFSO networks, multiplexing in wavelength [4], polarization [5], intensity [6], code [7], and phase [8] dimensions have been reported in the past literature. Mode division multiplexing (MDM) is a new technology for transmitting information, capitalising on the dimension of Eigen mode for intensifying data transmission rates in optical links. Different techniques including optical signal processing [9], spatial light modulator [10], photonic crystal fiber [11], few-mode fiber [12] and modal decomposition techniques [13] have been reported to transmit distinct data signals on generated laser modes in MDM systems. The research study in [14] represents the successful transmission of 5 Gbps-20 GHz data at FSO link range of 500 m with two Hermite Gaussian (HG) modes i.e. HG00 and HG01 in clear weather conditions. The transmission of 5Gbps-10GHz information at 2.5 km by exploiting solid core fiber-based MDM of Laguerre Gaussian (LG) modes has been demonstrated in [15]. The transmission of 7.5 Gbps-15 GHz information over 2.5 km FSO link in clear weather conditions with the help of LG00, LG01, and LG02 beams is discussed in [16]. The research in [17] shows the information transmission of 5 Gbps-20 GHz over 14 km FSO link with the help of distinct HG modes and optical pre-amplification in clear weather conditions. The transmission of 5 Gbps - 20 GHz information using HG00 and LG00 beams in clear weather over 14 km FSO link incorporating alternate mark inversion (AMI) modulation has been discussed in [18]. In another work [19], the authors report a 3-channel MDM-based few-mode fiber link for triple-play services using differential phase-shift keying (DPSK) modulation scheme. The findings report

the transmission of 30 Gbps information over 1300 m fiber link. Investigations on hybrid wavelength division multiplexing (WDM)-MDM based FSO transmission system using duobinary and AMI modulation technique has been reported in [20]. The authors in [21] report the performance comparison of different amplifier configurations viz. inline, booster, and preamplifier in the high-speed MDM-based multimode fiber link. The findings indicate inline amplifier configuration demonstrates the best performance. The application of a double lens scheme in a 100 m/320 Gbps MDM-based FSO link has been discussed in [22]. The simulative investigation of $4 \times 4, 6 \times 6, and\ 9 \times 9$ multi-input multi-output (MIMO) MDM-based multimode fiber link over 90 km link range using linear polarized (LP) modes have been discussed in [23]. In another work [24], the authors report modeling and performance investigation of 10 Tbps hybrid WDM-MDM-based multimode fiber links for short reach applications using LP modes. The simulative investigation of hybrid MDM-Dense-WDM-based passive optical network services is discussed in [25]. The study in [26] demonstrates the modeling and analysis of the performance of 2×2 MIMO system employing hybrid MDM and mode group division multiplexing (MGDM) for transmission of millimeter-wave frequency signals.

The modulation scheme plays a significant role in the performance of information transmission systems. In this research, a comparison of performance for various modulation schemes viz., NRZ, AMI, and DPSK in a 2×2, 3×3, and 4×4 MIMO-MDM-based RoFSO transmission system is reported. This work is mainly motivated by the following key points: (1) Design of a long-haul high-speed spectrum-efficient RoFSO transmission system by using hybrid MIMO-MDM techniques, (2) performance analysis of NRZ, AMI, and DPSK modulation schemes in the proposed RoFSO transmission link and finding the optimal modulation scheme (3) to investigate proposed link performance in dynamic weather conditions. The novelty of the proposed MIMO-MDM-RoFSO transmission system is to design and analyse the performance of system in terms of several modulation schemes like AMI, DPSK and NRZ by incorporating distinct modes of HG profile under different weather conditions. It offers major improvement in information capacity and connectivity as compared to other existing system for long-reach and high data rate transmission The simulation setup and system parameters are explained in Section 2. In Section 3, results are presented and discussed, and in Section 4, the conclusion is given.

2. System design

Fig. 1 represents the RoFSO transmission system based on MIMO-MDM, that is developed with simulation software from Optisystem. In the proposed work, we have used HG modes of a laser to improve link data rate. HG modes have more advantages as for MDM, the HG modes are more flexible to atmospheric turbulence as compared to LG modes and as a result there is a considerable improvement in link reach achievabilty. Also for transmission system with limited antenna apertures, HG modes provide a higher achievable bit transmission rate and robusteness to beam rotation in contrast to LG modes.

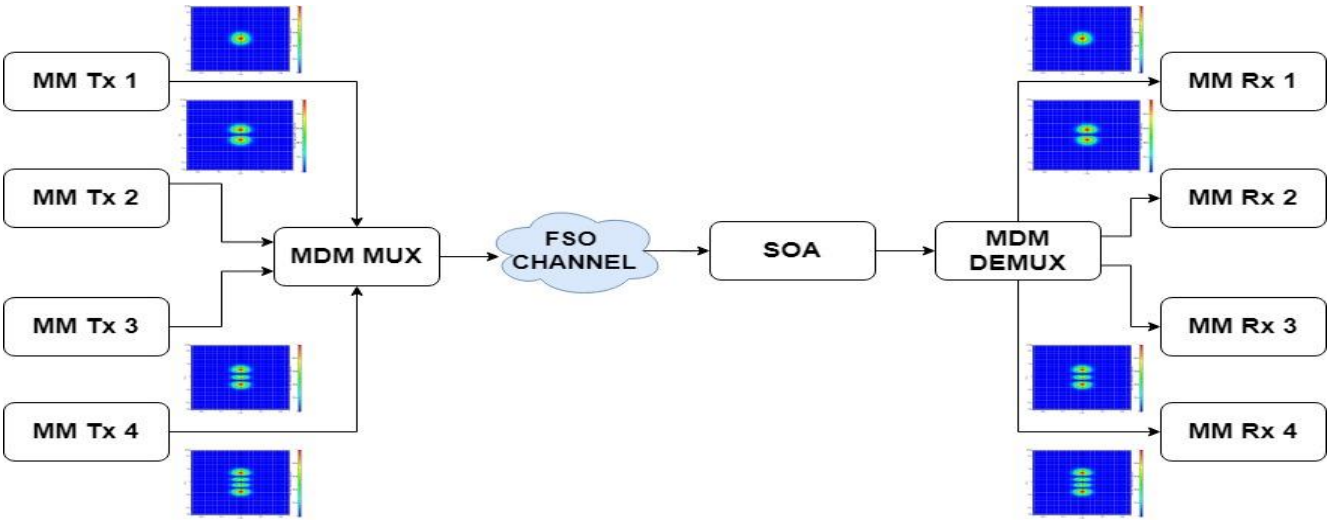

Fig. 1. RoFSO transmission system based on the proposed 4-channel MDM (color online)

Information source, a line encoder, an optical modulator, and an optical laser source are there in every multimode (MM) transmitter (Tx) block. Binary information is generated for each channel using a Pseudorandom bit sequence generator which with the help of line encoder is converted into an electrical signal. In NRZ line encoder '1' is transmitted via a one-bit light pulse. Delay-and-subtract and delay-and-add are employed in AMI encoders to produce AMI line codes [27, 28]. In order to generate the DPSK data sequence, the DPSK

encoder is precoded by a delay-XOR pre-coder to be modulated with the optical carrier [29]. The phase noise of the laser diodes used in transmitter section is -100 dBc/Hz. The electric field emitted in laser phase noise model can be expressed as:

$$e(t) = E.\exp[j(2\pi f_0 + \emptyset(t))] \quad (1)$$

where E is electric field amplitude, $\emptyset(t)$ is random process representing the phase noise and f_0 is the instantaneous-frequency fluctuation. This signal is then directed towards a Mach-Zehnder modulator that modulates it with a laser beam and a 20 GHz radio signal. In this work, the information signal from each transmitter block is transmitted using distinct HG modes which are expressed as [30]:

$$\varphi_{m,n}(r,\emptyset) = H_m\left(\frac{\sqrt{2}x}{\omega_{0,x}}\right)\exp\left(-\frac{x^2}{\omega_{ox}^2}\right)\exp\left(j\frac{\pi x^2}{\lambda R_{ox}}\right) \times H_n\left(\frac{\sqrt{2}y}{w_{o,y}}\right)\exp\left(-\frac{y^2}{w_{oy}^2}\right)\left(j\frac{\pi y^2}{\lambda R_{oy}}\right) \quad (2)$$

where $H_m\ and\ H_n$ are Hermite polynomials, ω_0 is the spot dimension, R is the curvature radius and m and n are x-axis and y-axis dependencies respectively. A continuous wave (CW) laser signal having a launch power of 0 dBm along with a multimode generator are employed in the proposed link for multimode generation. The information signal from each transmitter block is then directed towards an MDM multiplexer (MUX) for multiplexing all the channels. As per by ITU specifications for MUX/DEMUX with 100 GHz channel spacing, the minimum insertion loss for practical MUX/DEMUX is 0.3 dB with the bandwidth of 15 GHz. This results in negligible signal loss in the link and hence considered as ideal MUX/DEMUX. This signal is then propagated in free air by means of transmitter lens. The FSO link equation is [31]:

$$P_{Received} = P_{Transmitted}\left(\frac{d_R^2 Z}{(d_T+\theta Z)^2}\right)10^{-\sigma Z/10} \quad (3)$$

where d_T and d_R are the aperture size of transmitter and receiver lens respectively, θ is the size of optical beam (divergence angle), Z is the range of data transmission and σ is the weather specific attenuation constant. The parameters of the simulation are shown in Table 1. A 0.1-A semiconductor optical amplifier (SOA) amplifies the optical signal at the input of the receiver followed by MDM de-multiplexer (DEMUX) that will de-multiplex various modes [32,33]. NRZ and AMI data signals are decoded using fixed threshold detection technique. For DPSK encoded signal demodulation, Mach-Zehnder interferometer having 1-bit delay is deployed [29]. A spatial avalanche photodiode (APD) is employed in each multimode receiver (Rx) block for optical to electrical signal conversion. SOA are important optical switching devices as of their high-speed switching speed and the ability to attain a high extinction ratio. Integrated arrays high-extinction ratio SOA gates probably offer a platform for large cross-connect array with switching speed for assuredly usage in optical packet burst and packet switching. SOA noise figure can be expressed as

$$NF = 2nK \quad (4)$$

$$K = \frac{(1+RG)(G-1)\delta g}{(1-R)G(\delta g-\alpha)} \quad (5)$$

where n is effective population parameter. For achieving low NF, n should be equal to 1. R and G represent residual reflectivity and gain respectively. δg and α represent the material gain and loss coefficient respectively.

Table 1. Simulation parameters [17, 18]

Parameter name	**Value**
SOA injection current	0.1 A
Operating wavelength	1550 nm
Laser line width	10 MHz
Bit rate/channel	10 Gbps
Transmission power	0 dBm
Ionization ratio	0.9
Dark current	10 nA
Responsivity of Photodiode	1 A/W
Power density thermal noise	1e-022 W/Hz
Avalanche photodiode gain	3
Beam divergence	0.25 mrad
Aperture diameter of Transmitter/Receiver antenna	10 cm

Under various fog weather conditions, atmospheric attenuation is calculated with the help of the equation [34]:

$$\beta(\lambda) = \frac{3.91}{V}\left(\frac{\lambda}{550}\right)^{-p} \quad (6)$$

where $\lambda\,(nm)$ is the wavelength, V (km) represents visibility range, and p represents the scattering coefficient, which is determined using Kim model as [35]:

$$p = \begin{cases} 0 & V < 0.5 \\ V - 0.5 & 0.5 < V < 1 \\ 0.16\,V + 0.34 & 1 < V < 6 \\ 1.3 & 6 < V < 50 \\ 1.6 & V > 50 \end{cases} \quad (7)$$

The attenuation is 16, 12, 9, and 0.14 dB/km for heavy, moderate, light fog and clear weather conditions respectively [15-18]. (In this work, we have considered weak atmospheric turbulence conditions with refractive index parameter $C_n^2 = 5 \times 10^{-17} m^{-2/3}$). Pointing error restricts the performance of atmospheric FSO systems. The pdf of pointing error mode is given as follows:

$$f(X) = \frac{\epsilon^2}{A^{\epsilon^2}} X^{\epsilon^2 - 1}, 0 \le X \le A = [\text{erf}(\vartheta)]^2 \quad (8)$$

where $\epsilon = w_L/2\sigma$ is the ratio of equivalent beam radius and pointing error jitter. $A_0 = [erf(v)]^2$ represents the composed power fraction at radius r=0.

In the proposed system, combined effect of attenuation for varied weather, atmospheric turbulence modelled using Gamma-Gamma (GG) distribution model with pointing error and geometric loss have been described numerically to investigate the channel gain. The channel gain, h of the proposed system is given by:

$$h = h_l h_p h_a \quad (9)$$

where deterministic path loss is represented by h_l, the fading due to geometric spread and pointing errors is represented by h_p and fading due to atmospheric turbulence is represented by h_a. Now, the primary FSO link equation under different attenuation effects is given by:

$$P_r = P_t . \left(\frac{A_r}{(\theta Z)^2}\right) . h_l \quad (10)$$

where the atmospheric path loss h_l, is given by:

$$h_l = exp(-\alpha Z) \quad (11)$$

where α is dependent on the rain, haze, or fog appearance. Further, the PDF of GG channel distribution is given as:

$$f_{h_a}(h_a) = \frac{2(pq)^{\left(\frac{p+q}{2}\right)}}{\Gamma(p)\Gamma(q)} . h_a^{\left(\frac{p+q}{2}\right)-1} K_{p-q}\left[2(pqh_a)^{\frac{1}{2}}\right] \quad (12)$$

3. Results and discussion

Fig. 2 (a)-(c) presents SNR curves with incrementing FSO range for a 2×2 MDM-based RoFSO transmission system in clear weather conditions using NRZ, AMI, and DPSK modulation scheme respectively. From the findings shown in Fig. 2, it is demonstrated that with incrementing range, the received signal quality and overall link performance degrades for the three modulation schemes. For NRZ, the maximum range with acceptable performance (SNR > 20 dB) is 20 km for channel 1 (HG00 mode) and 17 km for channel 2 (HG01 mode), whereas for the AMI modulation scheme, the maximum range is reported as 23 km for channel 1 and 20 km for channel 2. On the other hand, for the DPSK modulation scheme, the maximum supported range is 32 km for channel 1 and 28 km for channel 2.

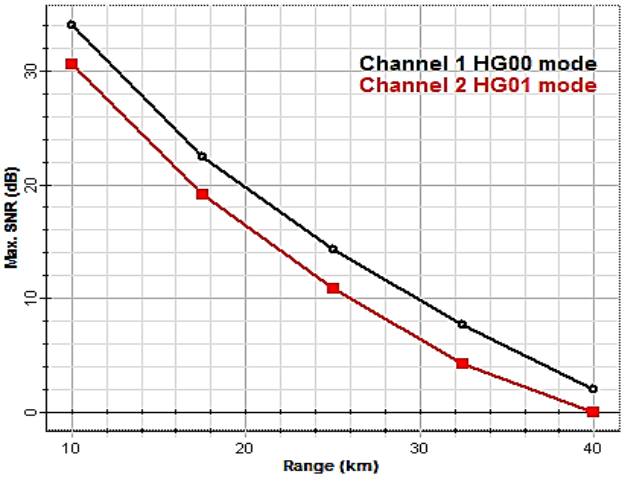

(a)

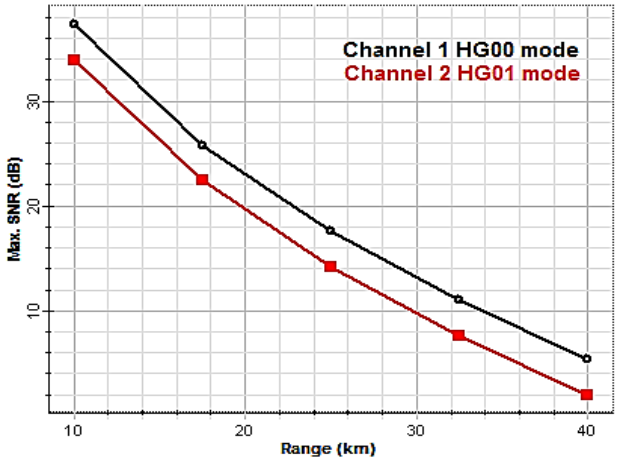

(b)

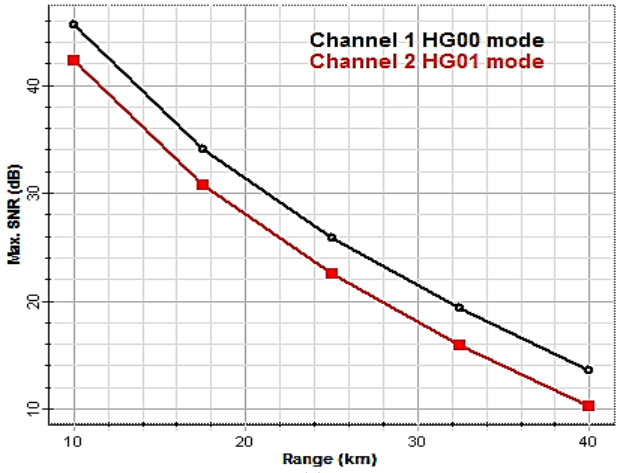

(c)

Fig. 2. SNR v/s FSO link range for 2×2 MDM-RoFSO transmission system using (a) NRZ, (b) AMI, (c) DPSK (color online)

Fig. 3 (a)-(c) reports the SNR curves with incrementing FSO range for a 3×3 MDM-based RoFSO transmission system in clear weather using NRZ, AMI, and DPSK modulation scheme respectively. Fig. 3 demonstrates that for NRZ, the maximum performance link range is calculated as 17 km for channel 1 (HG00 mode), 14 km for channel 2 (HG01 mode), and 11 km for channel 3 (HG02 mode) whereas for AMI modulation scheme, the maximum link range is calculated as 19 km for channel 1, 17 km for channel 2, and 13 km for channel 3. Alternatively, for the DPSK modulation scheme, 28 km for channel 1, 24 km for channel 2, and 19 km for channel 3 is the maximum computed link range.

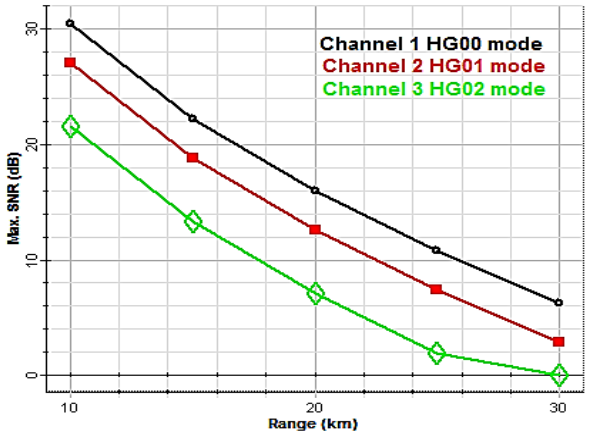

(a)

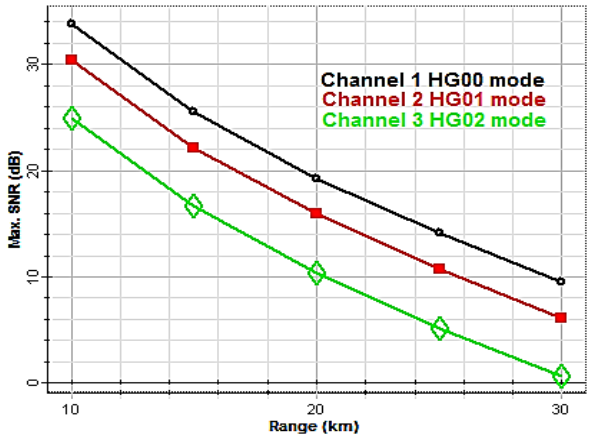

(b)

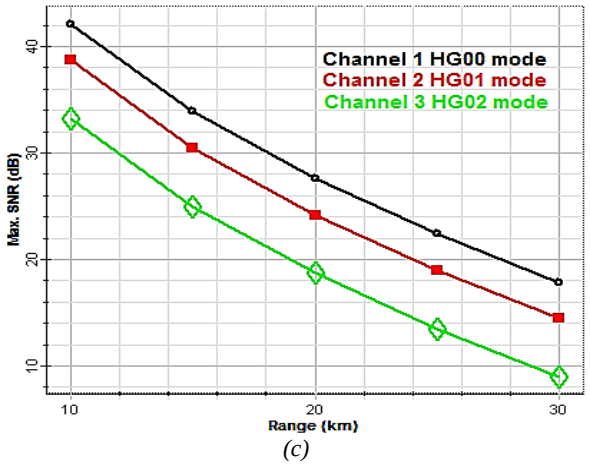

(c)

Fig. 3. SNR v/s FSO link range for 3×3 MDM-RoFSO transmission system using (a) NRZ, (b) AMI, (c) DPSK (color online)

Fig. 4 (a)-(c) reports SNR curves as FSO link range function in clear weather conditions for a 4×4 MDM-based RoFSO transmission system with the help of NRZ, AMI, and DPSK modulation schemes respectively. The results illustrate that for the NRZ modulation scheme, the maximum supported acceptable performance link range is reported as 15 km for channel 1 (HG00 mode), 12.5 km for channel 2 (HG01 mode), 9.5 km for channel 3 (HG02 mode), and 9 km for channel 4 (HG03 mode) whereas for AMI modulation scheme, maximum link range is reported as 16 km for channel 1, 13.5 km for channel 2, 10.3 km for channel 3, and 9.8 km for channel 4. Also, for the DPSK modulation scheme, the maximum link range is reported as 24 km for channel 1, 21.5 km for channel 2, 17 km for channel 3, and 16 km for channel 4.

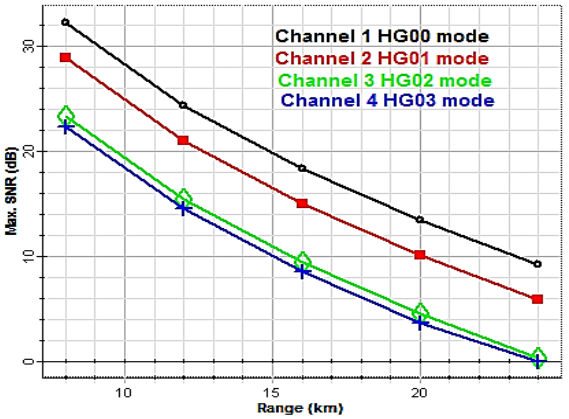

(a)

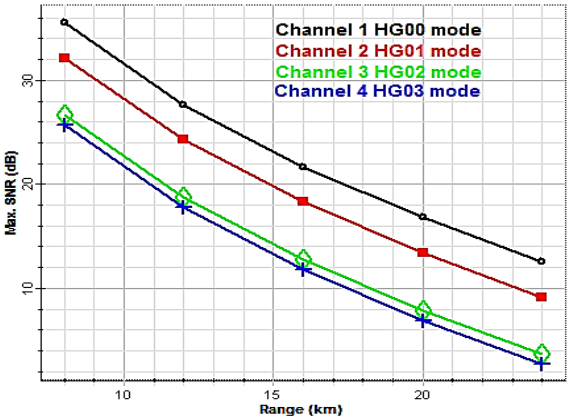

(b)

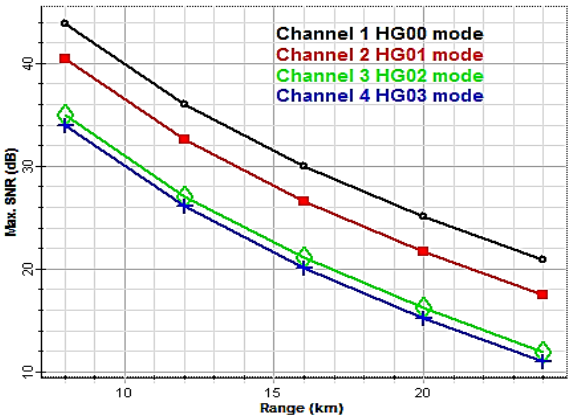

(c)

Fig. 4. SNR v/s FSO link range for 4×4 MDM based RoFSO transmission system using (a) NRZ, (b) AMI, (c) DPSK (color online)

From the results in Figs. 2-4, the best performance of all MIMO-MDM-based RoFSO transmission systems is reported by the DPSK modulation scheme, followed by AMI and NRZ scheme. The reason is the transmission of the information signal in DPSK modulation by varying carrier signal phase rather than amplitude. Hence, the atmospheric attenuation effect on the DPSK signal is significantly less [29]. The analysis illustrated that the maximum supported link range for all channels deploying 40 Gbps - 80 GHz MDM-RoFSO system based on the proposed DPSK modulation scheme with acceptable SNR ($> 20\,dB$) is 16 km under clear weather. It is observed that HG00 mode performs best for all modulation schemes, followed by HG01, HG02, and HG03. This shows that HG00 mode is most robust and least affected by channel fading.

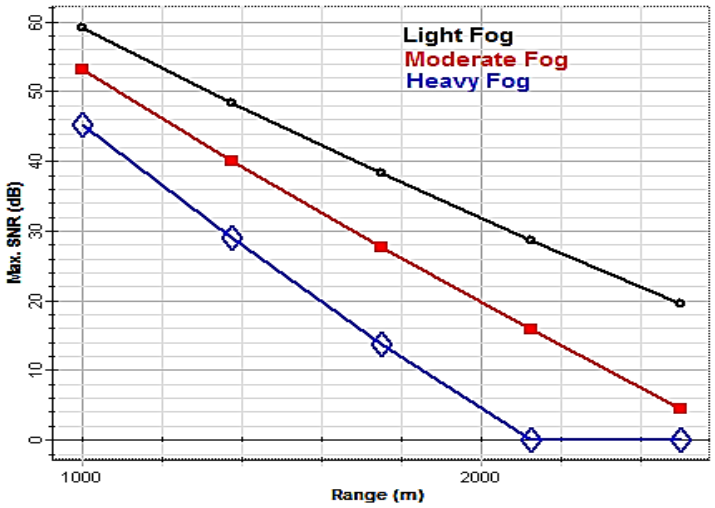

(a)

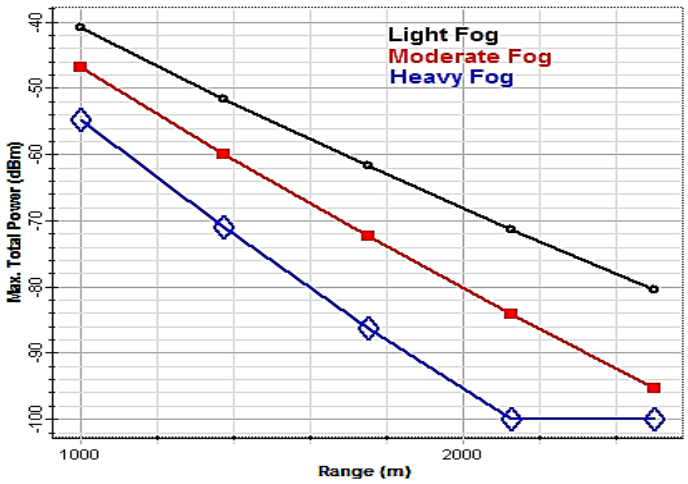

(b)

Fig. 5. (a) SNR (b) Power v/s FSO link range in various fog weather using MDM-RoFSO transmission system based on DPSK modulation scheme (color online)

In this study, we also report the proposed 40Gbps-80GHz MDM-RoFSO system performance under different fog conditions. Fig. 5 records SNR and received power curves with incrementing FSO range under various conditions of fog. The signal SNR is calculated as 59.21, 38.25, and 19.55 dB in light fog; 53.39, 27.79, and 4.95 dB in moderate fog; and 45.61, 13.77, and 0 dB in heavy fog at 1000, 1750 and 2500 m respectively. Further total signal power is calculated as -40.78, -61.74, and -80.43 dBm in light fog; -46.81, -72.84, and -95.37 dBm in moderate fog; and -54.93, -86.23, and -100 dBm in heavy fog at 1000, 1750 and 2500 m respectively. The findings of this research represent an acceptable SNR link range of 1600 m in heavy fog conditions, which increases to 2000 m in moderate fog and 2500 m in light fog conditions. Fig. 6 shows eye diagrams of the received signals for different fog weather at appropriate achievable range. Table 2 tabulates a comparative performance analysis of the proposed RoFSO transmission system employing HG-MDM and DPSK signals with previous literature works.

Table 2 shows that in terms of maximum information capacity and link reach, the proposed link performs best compared to the existing works.

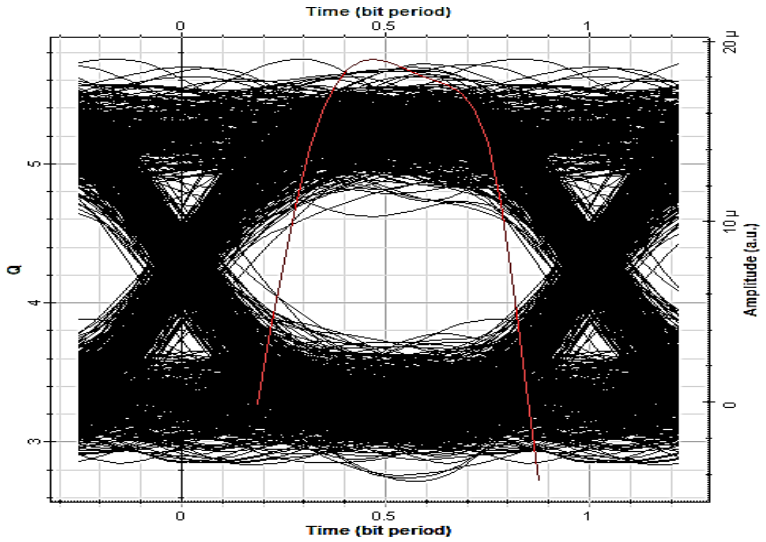

(a)

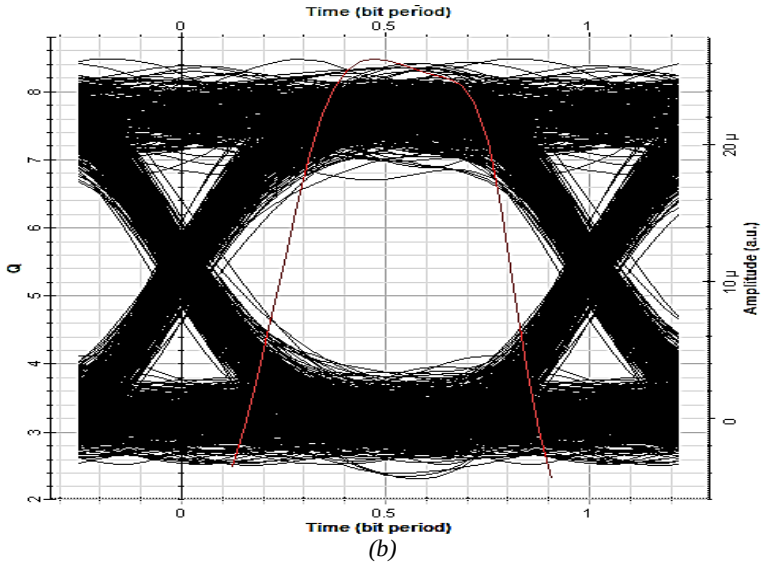

(b)

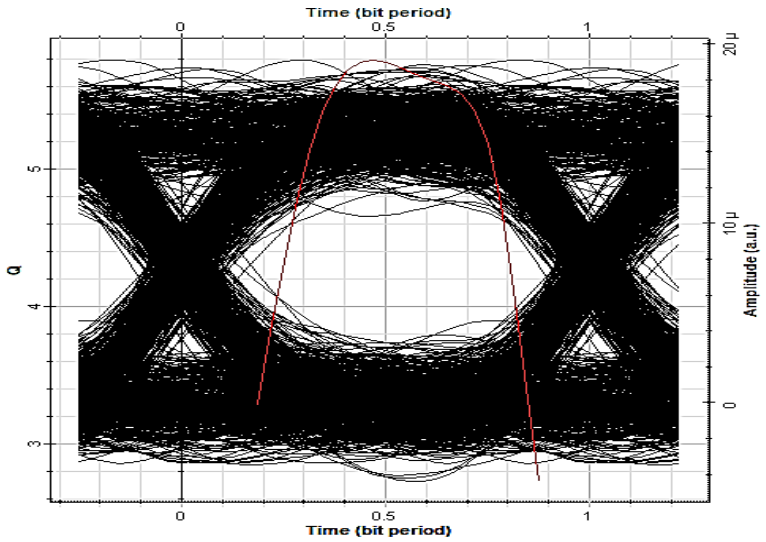

(c)

Fig. 6. Eye diagram for (a) light fog (2.5 km); (b) moderate fog (2 km); (c) heavy fog (1.6 km)

Table 2. Comparison of the performance for proposed DPSK-based MDM-RoFSO transmission system with existing works

Reference Work	Method/Technique	Information rate	Weather condition	Maximum link reach
Ref [14]	MDM-RoFSO using HG modes	5 Gbps	Clear	0.5 km
Ref [15]	Solid core-PCF based MDM-RoFSO system with NRZ. Encoding	5Gbps	Clear	2.5 km
			Thin fog	0.6 km
			Thick fog	0.4 km
			Heavy fog	0.2 km
Ref [16]	MDM-RoFSO system using LG beams with NRZ encoding	7.5Gbps	Clear	2.5 km
			Thin fog	0.6 km
			Thick fog	0.4 km
			Heavy fog	0.2 km
Ref [17]	MDM of spiral phase HG modes with NRZ. Encoding	5Gbps	Clear	14 km
			Moderate fog	1.4 km
			Heavy fog	1.1 km
Ref [18]	MDM of HG modes with AMI encoding	5Gbps	Clear	14 km
Proposed work	MDM of HG modes with DPSK encoding	40Gbps	Clear	16 km
			Light fog	2.5 km
			Moderate fog	2 km
			Heavy fog	1.6 km

4. Conclusion

In this article, we demonstrate NRZ, AMI and DPSK modulation schemes performance comparison in a 2×2, 3×3, and 4×4 MIMO-MDM-based RoFSO transmission system in clear weather conditions. Based on these findings, it is inferred that for all MIMO-MDM-based RoFSO systems, DPSK modulation performs significantly better than other modulation schemes. These results show that within the acceptable performance limits (i.e. SNR > 20 dB), the maximum link range for the proposed 40 Gbps - 80 GHz MDM-RoFSO link by integrating the DPSK modulation scheme under clear weather conditions is 16 km. The range reduces to 1.6 km under heavy fog, 2 km under moderate fog and 2.5 km under light fog conditions, which is a considerable improvement compared to the existing works. In future works, hybrid polarization division multiplexing and WDM techniques will further enhance the proposed link information capacity.

References

[1] M. A. Khalighi, M. Uysal, IEEE Communications Surveys & Tutorials **16**(4), 2231 (2014).
[2] A. Mahdy, J. S. Deogun, Proceedings of IEEE Wireless Communications and Networking Conference **4**, 2399 (2004).
[3] Sushank Chaudhary, Xuan Tang, Xian Wei, AEU – International Journal of Electronics and Communications **93**, 208 (2018).
[4] H. Zhou et al., Wireless Communications and Networking Conference (WCNC) 2677 (2014).
[5] Xuan Tang, Zabih Ghassemlooy, Sujan Rajbhandari, Wasiu O. Popoola, Chung Ghiu Lee, Journal of Lightwave Technology **30**(16), 2689 (2012).
[6] A. Kanno et al., Optics Express **19**, B56 (2011).
[7] H. Al-Khafaji et al., Journal of the European Optical Soc. - Rapid Publications **8**, 13022 (2013).
[8] C. B. Naila et al., Optical Engineering **50**, 105006 (2011).
[9] A. Amphawan, Optics Express **19**, 9056 (2011).
[10] S. Ö. Arık et al., J. Lightw. Technol. **34**, 2867 (2016).
[11] A. Amphawan et al., Journal of Modern Optics **60**, 1675 (2013).
[12] Y. Jung et al., Optics Express **21**, 24326 (2013).
[13] J. Carpenter et al., Optics Express **22**, 96 (2014).
[14] A. Amphawan, S. Chaudhary, Proc. of SPIE **9524**, 95242H-1-6 (2015).
[15] Sushank Chaudhary, Angela Amphawan, Photonic Network Communications **36**, 263 (2018).
[16] Sushank Chaudhary, Angela Amphawan, Laser Physics **28**(7), 075106-1-9 (2018).
[17] Sushank Chaudhary, Angela Amphawan, Photonic Network Communications **35**, 374 (2018).

[18] Sushank Chaudhary, Angela Amphawan, International Journal of Electronics Letters **7**(3), 304 (2019).
[19] Amphawan Angela, Najm Mustafa, Proc. Of 8th IEEE International Conference on Control System, Computing, and Engineering, Peang, Malaysia 244 (2018).
[20] Zhou Zhenlei, Li Erkai, Zhang Haigiang, Journal of Optical Communications, DeGryyter, article in press. (2019).
[21] Rajan Gupta, R. S. Kaler, Optical Engineering **55**(5), 056102-1-6 (2016).
[22] Li Chung-Li et al., Laser Physics Letters **13**(2016), 075201-1-6, (2016).
[23] Rajan Gupta, R. S. Kaler, Optoelectron. Adv. Mat. **11**(11-12), 643 (2017).
[24] Rajan Gupta, R. S. Kaler, Optoelectron. Adv. Mat. **12**(7-8), 441 (2018).
[25] Fazea Yousuf, Optik **183**, 994 (2019).
[26] A. Raza, S. Ghafoor, M. F. U. Butt, Photon. Netw. Commun. **35**, 265 (2018).
[27] O. Leclerc, B. Lavigne, E. Balmefrezol, P. Brindel, L. Pierre, D. Rouvillain, F. Seguineau, Journal of Lightwave Technology **21**, 2779 (2009).
[28] P. J. Winzer, R.-J. Essiambre, Proceedings of the IEEE **94**, 952 (2006).
[29] G. Xie et al., IEEE International Conference on Communication (ICC), 1 (2011).
[30] A. Ghatak, K. Thyagarajan, An introduction to Fiber Optics, Cambridge University Press, Cambridge (1998).
[31] Z. Ghassemlooy, W. O. Popoola, Terrestrial Free Space Optical Communications, in Mobile and Wireless Communication Network Layer and Circuit Level Design, ed. By S. A. Fares, F. Adachi (InTech, 2010).
[32] A. Mourka et al., Scientific Reports **3**, 1422-1-8 (2013).
[33] A. Amphawan et al., IEEE Int. Conf. Photon. (ICP), IEEE, Langkawi, 1-5 (2010).
[34] D. R. Kolev, K. Wakamori, M. Matsumoto, J. Lightwave Technol. **30**, 3727 (2012).
[35] I. Kim, B. Mcarthur, E. Korevaar, Proc. of SPIE Optical Wireless Communication **6303**, 1 (2006).

*Corresponding author: mehtab91singh@gmail.com